

Estimation of the cosmic ray mass composition at energy above 10^{17} eV according to scintillation detectors of Yakutsk array

A. V. Glushkov & A. Sabourov

tema@ikfia.ysn.ru

Yu. G. Shafer Institute of Cosmophysical Research and Aeronomy SB RAS

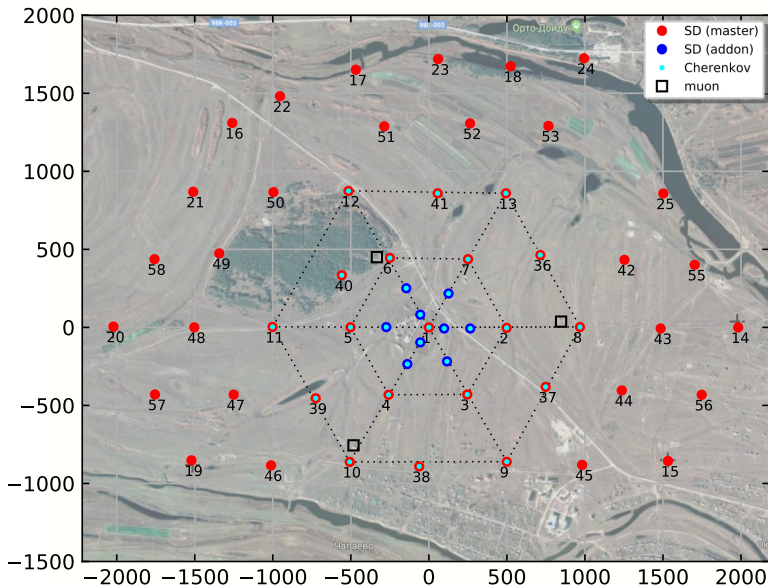
ISCRA 2019 — International Symposium on Cosmic Rays and Astrophysics
25–28 June 2019, MePHI, Moscow

Energy spectrum and mass composition of UHECR are crucial for solving the puzzle of their origin, acceleration and propagation in the Universe. The only method of observing them is EAS registration.

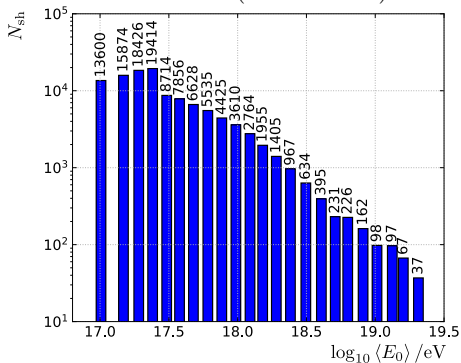
At the Yakutsk EAS array the mass composition is estimated by the parameters of lateral distribution functions of different EAS components.

$$\langle \log A \rangle = \frac{x_{\max}^{\text{p}} - x_{\max}^{\text{exp.}}}{x_{\max}^{\text{p}} - x_{\max}^{\text{Fe}}}, \quad (1)$$

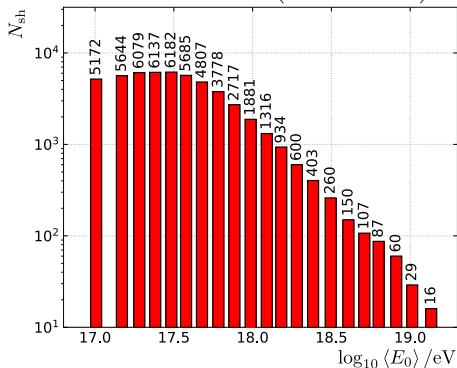
Experimental data



SD: 124052 events (1977 - 2017)



Muons: 52044 events (1986 - 2017)



- $E_0 \geq 10^{17}$ eV
- $\theta \leq 38.7^\circ$ $\langle \cos \theta \rangle \simeq 0.90$
- 1 km around the center: 6 *Trigger-500* triangles + 6 *Trigger-1000* triangles
- $\sigma(\text{axis}) \leq 30$ m *Trigger-500*
- $\sigma(\text{axis}) \leq 50$ m *Trigger-1000*

$$E_0 = (3.76 \pm 0.3) \times 10^{17} \cdot \rho_s(600)^{1.02 \pm 0.02}$$

SD mean density:

$$\langle \rho_s(r_i) \rangle = \frac{\langle E_0 \rangle}{E_0} \times \sum_{k=1}^N \frac{\rho_k(r_i)}{N}$$

Muon mean density:

$$\langle \rho_\mu(r_i) \rangle = \sum_{n=1}^{N_1} \frac{\rho_{\mu,n}(r_i)}{N_1 + N_0}$$

SD signal approximation:

$$\rho_s(r) = f_s(r) \cdot \left(\frac{600 + r_2}{r + r_2} \right)^{10},$$

$$f_s(r) = \rho_s(600) \times \left(\frac{600 + r_1}{r + r_1} \right)^a \times$$

$$\times \left(\frac{600 + r_M}{r + r_M} \right)^{b-a}$$

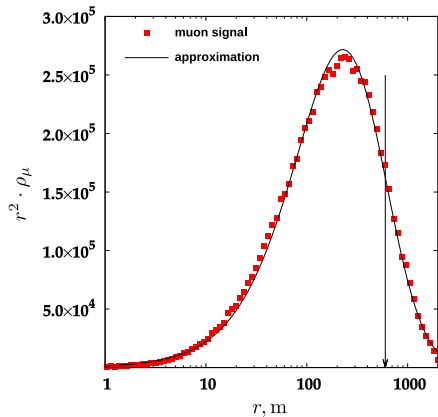
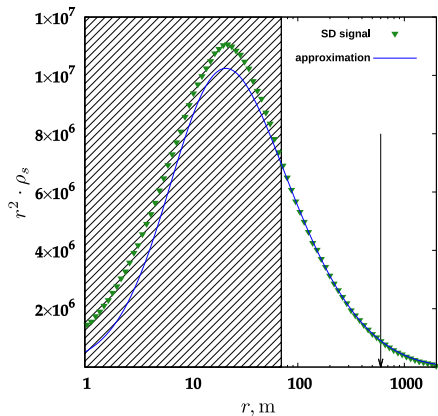
Muon signal approximation:

$$\rho_\mu(r) = f_\mu(r) \times \left(\frac{2000 + 600}{2000 + r} \right)^{6.5},$$

$$f_\mu(r) = \rho_\mu(600) \times \left(\frac{600}{r} \right)^{0.75} \times$$

$$\times \left(\frac{r_0 + 600}{r_0 + r} \right)^{b_\mu - 0.75}$$

Scintillation detectors signal



Within the framework of 2-components model:

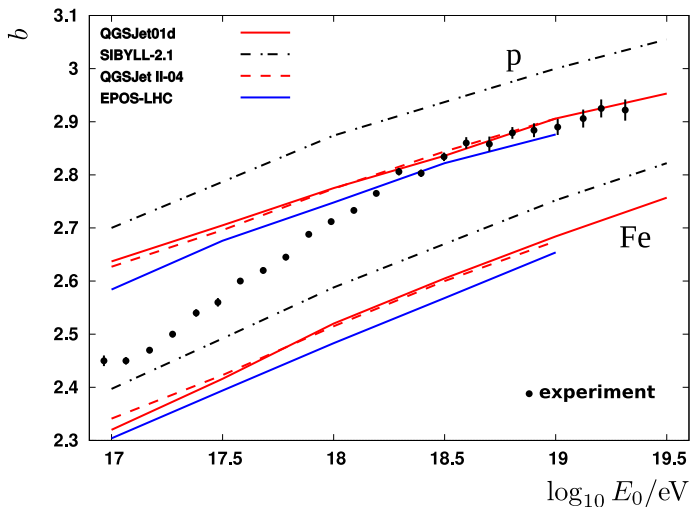
$$\begin{aligned}\langle \log A \rangle &= w_p \cdot \log 1 + w_{\text{Fe}} \cdot \log 56, \\ w_p &= 1 - w_{\text{Fe}}, \\ w_{\text{Fe}} &= \frac{\langle \log A \rangle}{\log 56}.\end{aligned}\tag{2}$$

In this case:

$$w_{\text{Fe}} = \frac{d_{\text{exp}} - d_p}{d_{\text{Fe}} - d_p},\tag{3}$$

Here d — any parameter that is sensitive to CR mass composition.

d is essentially the steepness of the SD LDF:



$$\eta = \rho_{\mu}(300)/\rho_s(300)$$

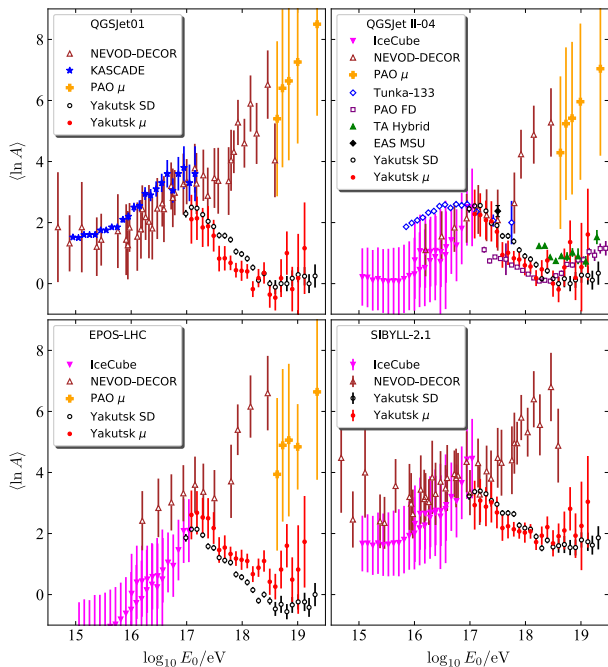
Corresponding weight ratio (3):

$$w_{\text{Fe}} = \frac{\log \eta_{\text{exp.}} - \log \eta_{\text{p}}}{\log \eta_{\text{Fe}} - \log \eta_{\text{p}}} = z$$

This is the z -scale factor, introduced in [EPJ Web of Conf. **210**, 02004 (2019)]

From (2) follows:

$$\langle \log A \rangle = z \cdot \log 56 \quad (4)$$



here:

CASCADE(2001),
Tunka-133(2014),
PAO FD(2017),
TA Hybrid(2019)

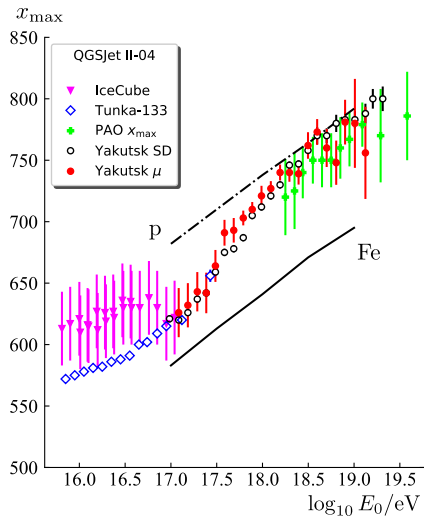
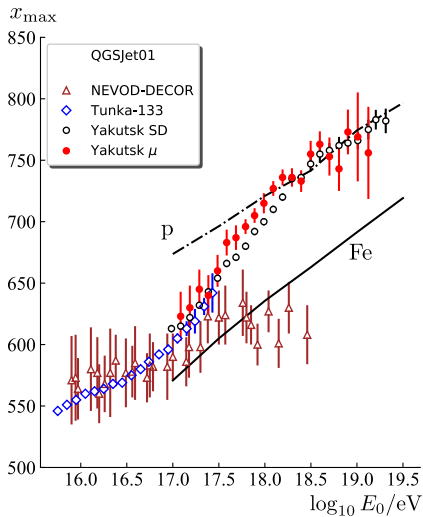
IceCube,
NEVOD-DECOR,
EAS-MSU,
PAO (μ) — from
 z -scale factor [EPJ
Web of Conf. **210**,
02004 (2019)]

- sensitive to CR mass comp.
- common techniques: optical observations
 - strict requirements on atmospheric conditions + limited duty cycle

However, from (1) & (4) follows:

$$x_{\max} = x_{\max}^{\text{P}} - z \cdot (x_{\max}^{\text{P}} - x_{\max}^{\text{Fe}}), \quad (5)$$

where z can be obtained with different techniques.



Conclusions

- CR mass composition and x_{\max} were estimated based on the data of scintillation detectors
 - Full MC of muon detectors?
- QGSJet01 & QGSJet II-04: in energy range $(1 - 30) \times 10^{17}$ eV CR mass composition changes from nuclei of intermediate group to protons
 - Galactic-Extragalactic transition?
- NEVOD-DECOR: inclined events ($\theta \geq 60^\circ$) at $E_0 \geq 10^{17}$ eV, nearly horizontal ($\theta \geq 70^\circ$) at $E_0 \sim 10^{18}$ eV
- NEVOD-DECOR & PAO μ — features of used techniques?

Further investigation is required.

Thank you!



z -scale factor SD

E_0 , eV ($\times 10^{17}$)	qGSJet01		qGSJet II-04		EPOS-LHC		SIBYLL-2.1		N_{sh}
	z	err	z	err	z	err	z	err	
0.966	0.573	0.031	0.614	0.031	0.465	0.031	0.808	0.031	10932
1.016	0.625	0.025	0.636	0.025	0.535	0.025	0.842	0.025	13600
1.480	0.617	0.025	0.640	0.025	0.535	0.025	0.848	0.025	15874
1.910	0.565	0.025	0.595	0.025	0.488	0.025	0.826	0.025	18426
2.410	0.511	0.025	0.494	0.025	0.395	0.025	0.769	0.025	19414
3.050	0.467	0.025	0.476	0.025	0.384	0.025	0.739	0.025	8714
3.780	0.395	0.025	0.390	0.025	0.302	0.025	0.667	0.025	7856
4.770	0.393	0.025	0.390	0.025	0.280	0.025	0.560	0.025	6628
6.070	0.361	0.025	0.346	0.025	0.262	0.025	0.660	0.025	5535
7.670	0.262	0.025	0.245	0.025	0.166	0.025	0.568	0.025	4425
9.710	0.244	0.025	0.225	0.025	0.142	0.025	0.545	0.025	3610
12.30	0.205	0.025	0.200	0.025	0.100	0.025	0.535	0.025	2764
15.20	0.132	0.025	0.154	0.025	0.038	0.025	0.476	0.025	1955
19.10	0.028	0.025	0.040	0.025	-0.050	0.025	0.383	0.025	1405
24.20	0.082	0.030	0.105	0.030	0.000	0.030	0.446	0.030	967
31.30	0.000	0.060	0.040	0.060	-0.053	0.060	0.390	0.060	634
40.60	-0.028	0.070	0.000	0.070	-0.118	0.070	0.400	0.070	395
51.20	0.000	0.062	0.040	0.062	-0.081	0.062	0.410	0.062	231
63.10	0.000	0.065	0.000	0.065	-0.138	0.065	0.385	0.065	226
81.60	0.044	0.062	0.030	0.062	-0.086	0.062	0.387	0.062	162
103.0	0.074	0.066	0.069	0.066	-0.059	0.066	0.447	0.066	98
133.0	0.060	0.075	0.069	0.075	-0.059	0.075	0.432	0.075	97
160.0	0.000	0.078	0.029	0.078	-0.106	0.078	0.405	0.078	67
206.0	0.062	0.095	0.086	0.095	0.000	0.095	0.466	0.095	37

z -scale factor Muons

E_0 , eV ($\times 10^{17}$)	QGSJet01		QGSJet II-04		EPOS-LHC		SIBYLL-2.1		$N_{sh.}$
	z	err	z	err	z	err	z	err	
1.016	0.528	0.200	0.571	0.200	0.652	0.200	0.732	0.200	5172
1.480	0.534	0.180	0.562	0.180	0.670	0.180	0.770	0.180	5644
1.910	0.460	0.160	0.521	0.160	0.632	0.160	0.719	0.160	6079
2.410	0.560	0.165	0.589	0.165	0.708	0.165	0.824	0.165	6137
3.050	0.392	0.130	0.426	0.130	0.546	0.130	0.672	0.130	6182
3.780	0.206	0.105	0.234	0.105	0.364	0.105	0.544	0.105	5685
4.770	0.208	0.100	0.253	0.100	0.385	0.100	0.560	0.100	4807
6.070	0.170	0.060	0.208	0.060	0.333	0.060	0.534	0.060	3778
7.670	0.108	0.060	0.198	0.060	0.296	0.060	0.517	0.060	2717
9.710	0.106	0.082	0.149	0.082	0.286	0.082	0.508	0.082	1881
12.30	0.100	0.060	0.140	0.060	0.276	0.060	0.517	0.060	1316
15.20	-0.044	0.065	0.046	0.065	0.167	0.065	0.431	0.065	934
19.10	0.046	0.075	0.118	0.075	0.219	0.075	0.483	0.075	600
24.20	0.088	0.088	0.190	0.088	0.276	0.088	0.552	0.088	403
31.30	-0.090	0.108	0.000	0.108	0.106	0.108	0.421	0.108	260
40.60	-0.115	0.105	-0.048	0.105	0.065	0.105	0.478	0.105	150
51.20	0.045	0.155	0.132	0.155	0.206	0.155	0.526	0.155	107
63.10	0.250	0.180	0.341	0.180	0.400	0.180	0.702	0.180	87
81.60	-0.044	0.182	0.048	0.182	0.122	0.182	0.482	0.182	60
103.0	0.045	0.362	0.134	0.362	0.204	0.362	0.562	0.362	29
136.0	0.290	0.375	0.402	0.375	0.432	0.375	0.759	0.375	16